

Supporting Information

Alternative anodes for Na-O₂ batteries: the case of the Sn₄P₃ alloy

Juan Luis Gómez-Cámer^{1,#}, Idoia Ruiz de Larramendi², Marina Enterría^{1,Iñigo}

Lozano^{1,2}, Begoña Acebedo¹, Domitille Bordeau¹, Nagore Ortiz-Vitoriano^{1,3*}

¹Center for Cooperative Research on Alternative Energies (CIC energiGUNE), Basque Research and Technology Alliance (BRTA), Parque Tecnológico de Alava, Albert Einstein 48, 01510 Vitoria-Gasteiz, Spain.

²Departamento de Química Orgánica e Inorgánica, Universidad del País Vasco (UPV/EHU), P.O. Box 664, 48080 Bilbao, Spain.

³Ikerbasque, Basque Foundation for Science, María Díaz de Haro 3, 48013 Bilbao, Spain.

*Present address: Dpto. Química Inorgánica e Ingeniería Química, Instituto de Química Fina y Nanoquímica IUNAN, Universidad de Córdoba, Campus Universitario de Rabanales, Edificio Marie Curie, 14071 Córdoba (Spain).

E-mail: nortiz@cicenergigune.com.

INDEX

| | | |
|------------|-------|--------|
| Table S1 | | Page 3 |
| Figure S1 | | Page 4 |
| Figure S2 | | Page 4 |
| Figure S3 | | Page 4 |
| Figure S4 | | Page 5 |
| Figure S5 | | Page 5 |
| Figure S6 | | Page 5 |
| Figure S7 | | Page 6 |
| Figure S8 | | Page 6 |
| Figure S9 | | Page 6 |
| Figure S10 | | Page 7 |
| Figure S11 | | Page 7 |
| Figure S12 | | Page 8 |
| Figure S13 | | Page 8 |
| Figure S14 | | Page 9 |
| Figure S15 | | Page 9 |

Table S1. Cell parameters and Figures of Merit of the Le Bail refinements of Sn₄P₃ materials synthesized by modified methods A to I.

| Synthesis | a | b | c | Avg. Crystallite size (nm) | Rp (%) | Rwp (%) | Rexp (%) | Chi-2 | Global user- weighted chi-2 |
|-----------|-----------|-----------|----------|----------------------------------|-----------|------------|-------------|-------|--------------------------------|
| A | 3.975(2) | 3.975(2) | 35.4(2) | 15.3 ± 0.2 | 13.5 | 20.2 | 17.5 | 1.32 | 1.46 |
| B | 3.9707(7) | 3.9707(7) | 35.37(9) | 18.9 ± 0.3 | 15.1 | 23.2 | 17.2 | 1.83 | 1.90 |
| C | 3.971(1) | 3.971(1) | 35.4(1) | 15.7 ± 0.2 | 14.4 | 28.2 | 24.0 | 1.39 | 1.50 |
| D | 3.971(3) | 3.971(3) | 35.4(3) | 14.9 ± 0.1 | 15.4 | 23.6 | 19.4 | 1.48 | 1.56 |
| E | 3.975(3) | 3.975(3) | 35.4(2) | 13.3 ± 0.2 | 14.2 | 21.7 | 18.2 | 1.42 | 1.50 |
| F | 3.974(3) | 3.974(3) | 35.4(3) | 14.1 ± 0.1 | 13.3 | 20.0 | 17.3 | 1.33 | 1.45 |
| G | 3.972(3) | 3.972(3) | 35.4(3) | 14.9 ± 0.2 | 14.6 | 21.7 | 18.6 | 1.36 | 1.48 |
| H | 3.974(3) | 3.974(3) | 35.4(3) | 14.4 ± 0.1 | 13.4 | 20.6 | 17.4 | 1.39 | 1.46 |
| I | 3.974(3) | 3.974(3) | 35.4(3) | 14.4 ± 0.3 | 14.0 | 20.6 | 18.1 | 1.30 | 1.40 |

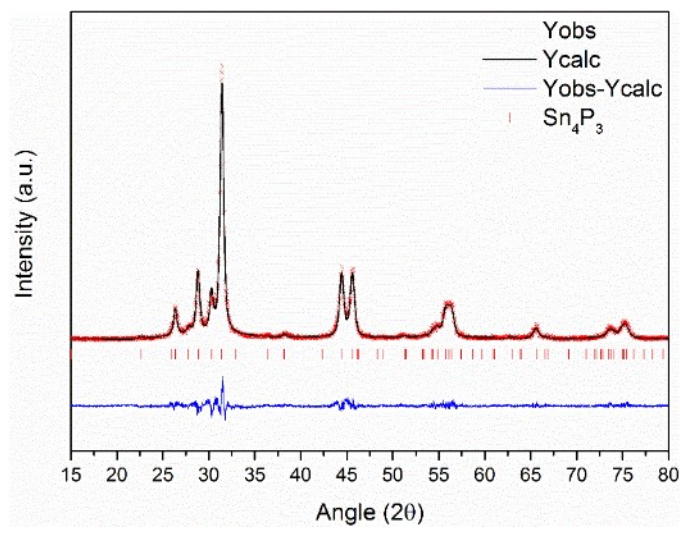


Figure S1. The XRD pattern along with the Le Bail refinement of Sn_4P_3 (synthesis A).

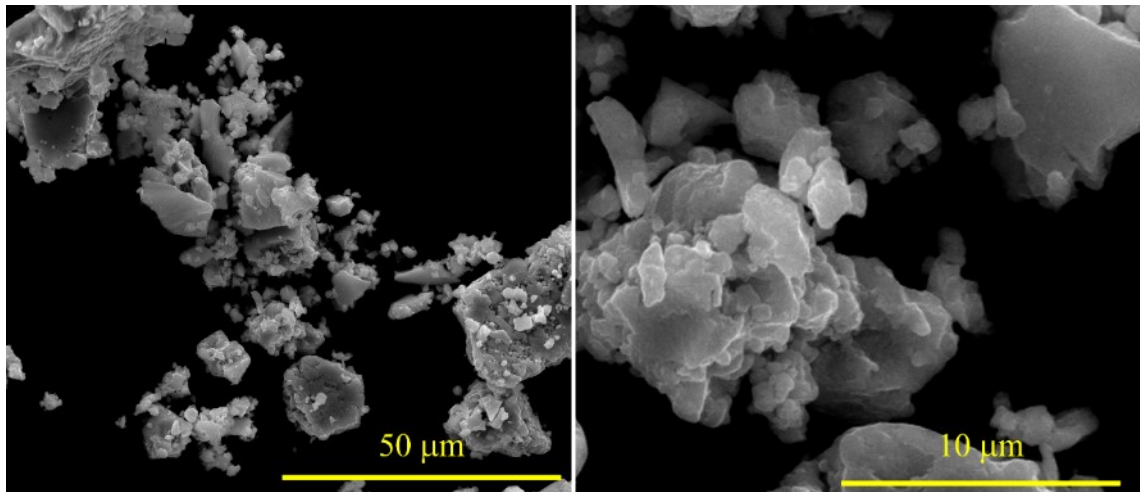


Figure S2. SEM images of the Sn_4P_3 powder from the original synthesis A.

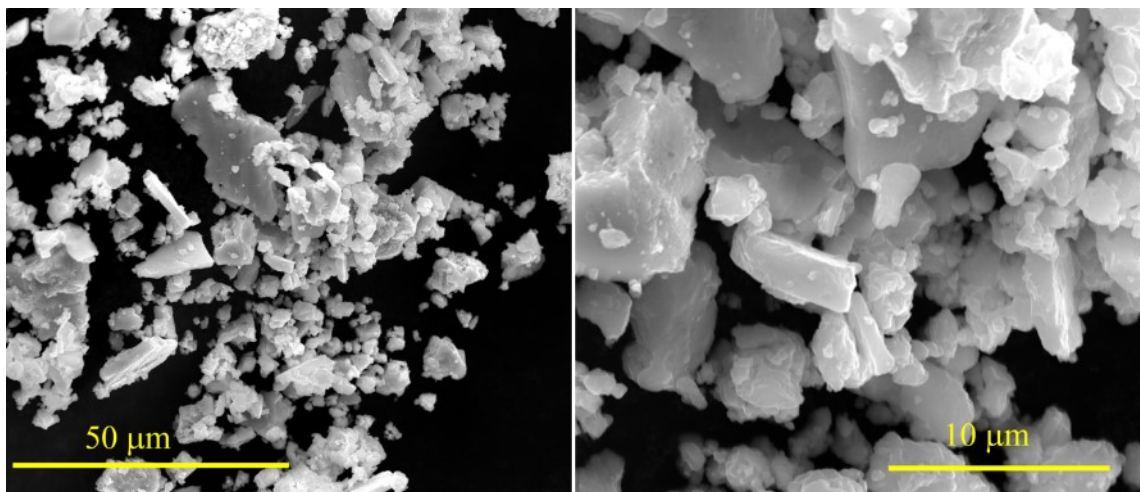


Figure S3. SEM images of the Sn_4P_3 powder from synthesis B.

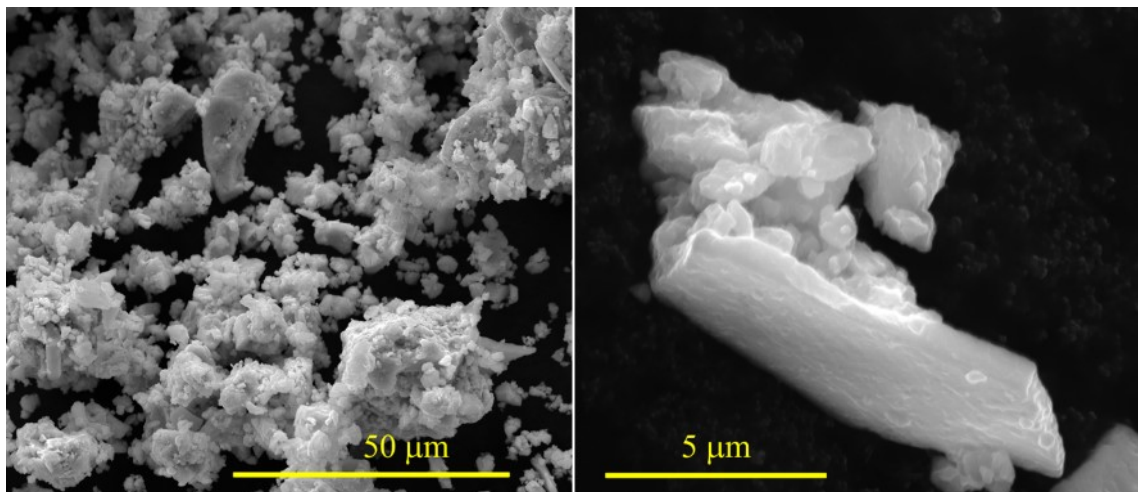


Figure S4. SEM images of the Sn₄P₃ powder from synthesis C.

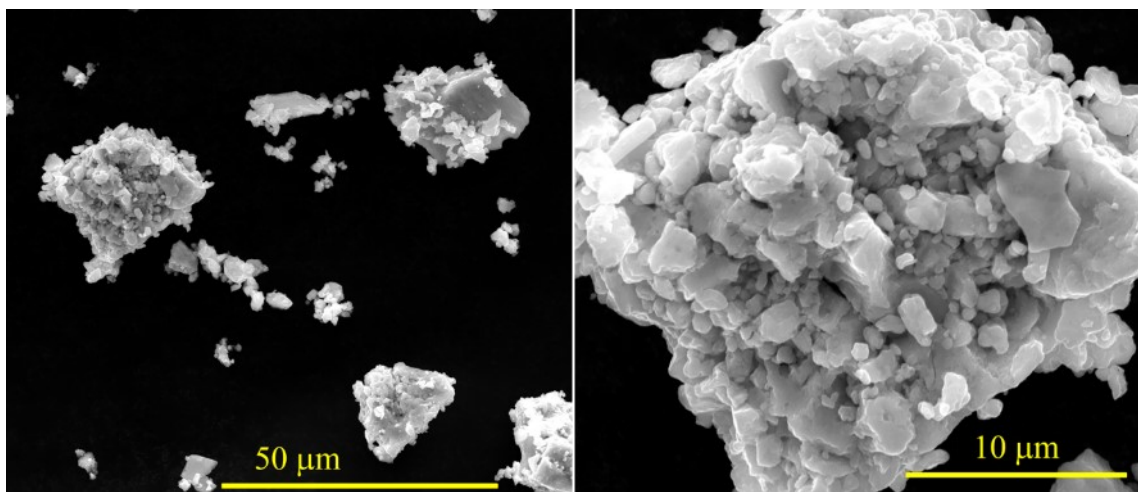


Figure S5. SEM images of the Sn₄P₃ powder from synthesis D.

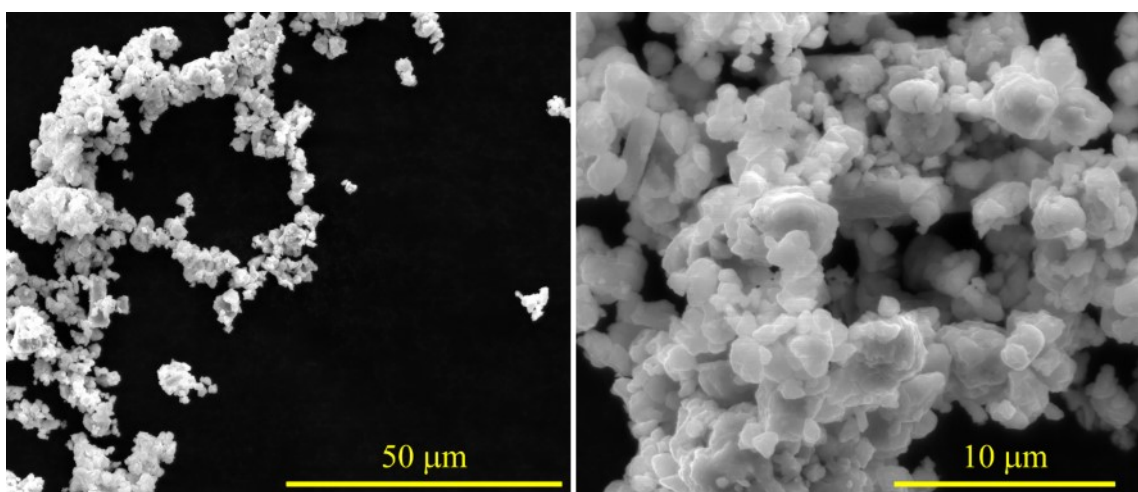


Figure S6. SEM images of the Sn₄P₃ powder from synthesis E.

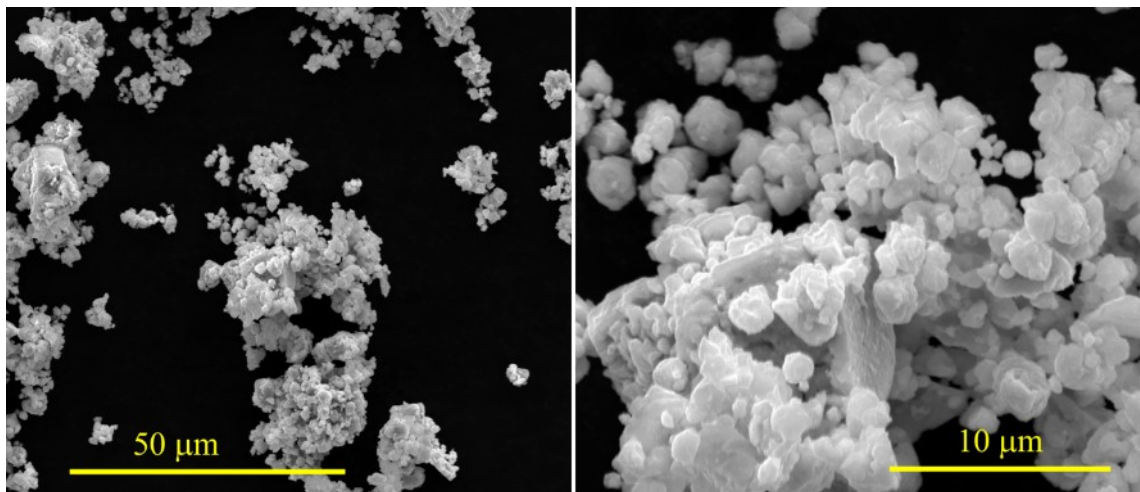


Figure S7. SEM images of the Sn₄P₃ powder from synthesis F.

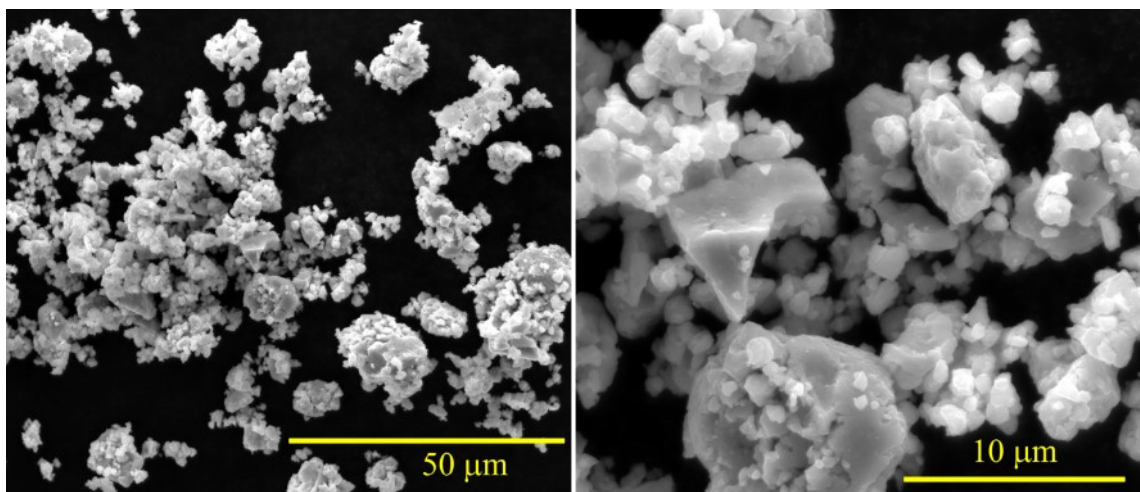


Figure S8. SEM images of the Sn₄P₃ powder from synthesis G.

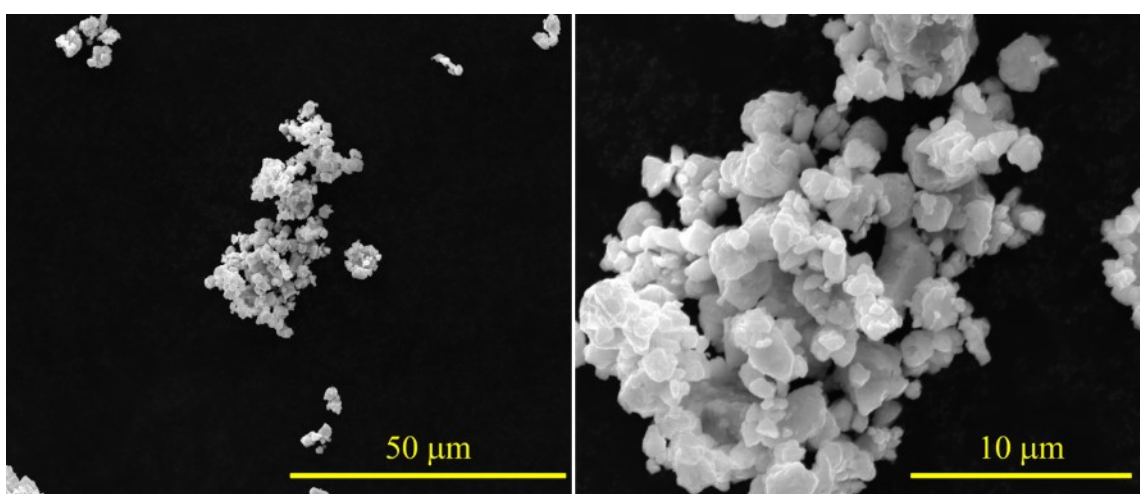


Figure S9. SEM images of the Sn₄P₃ powder from synthesis H.

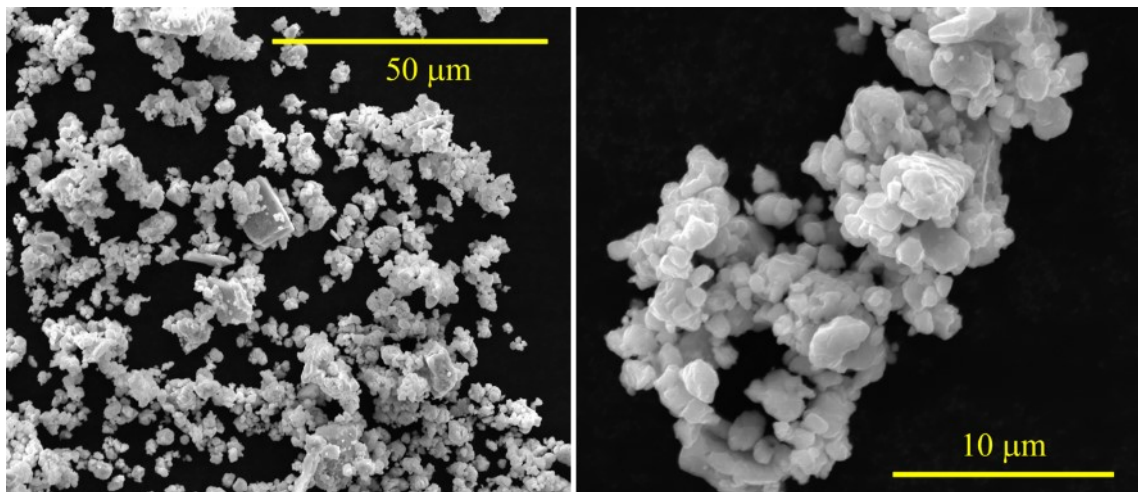


Figure S10. SEM images of the Sn₄P₃ powder from synthesis I.

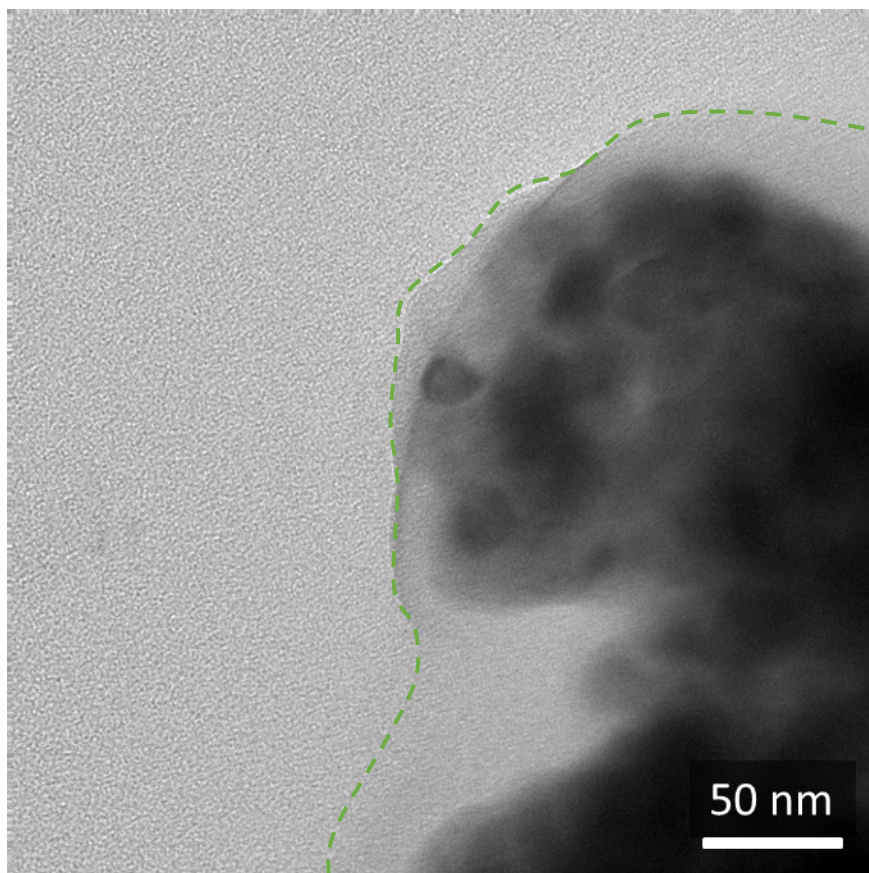


Figure S11. TEM image of the carbon coating resulting from the second milling step with Super C65 (synthesis A was used as a representative example to show carbon coating).

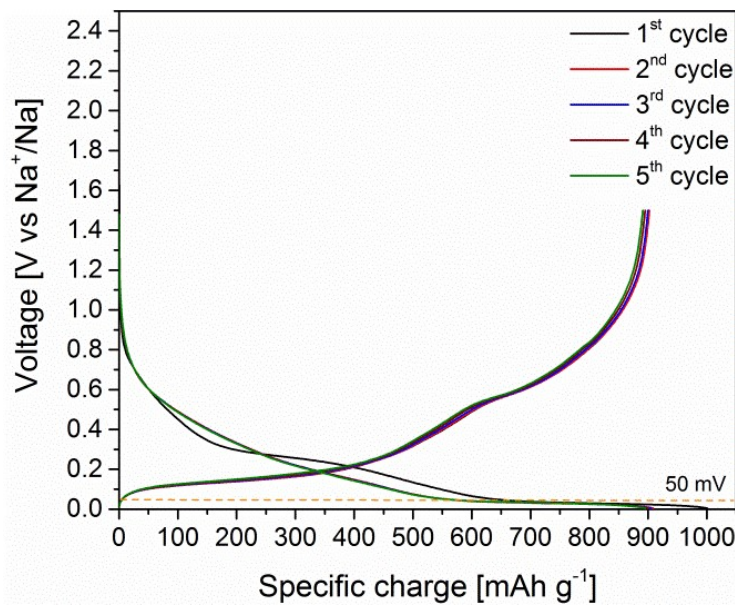


Figure S12. Galvanostatic charge-discharge curves of the five initial cycles of synthesis

A cycled with 5 mV cut-off at 100 mA g⁻¹ in a Na-ion battery. The dashed bar guides the eye to the limit of 50 mV.

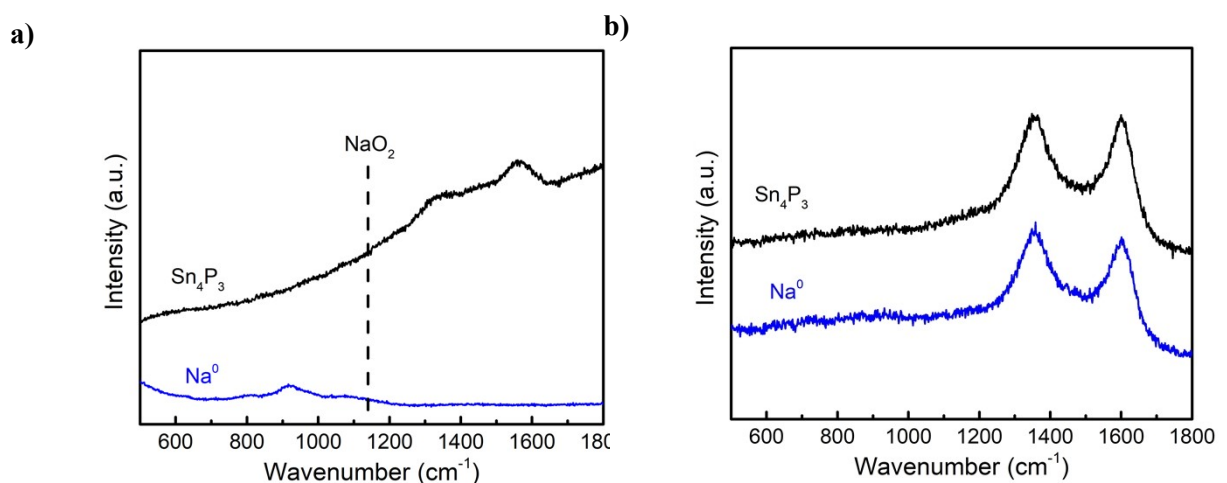


Figure S13. Raman spectra of a) metallic Na and Sn₄P₃/C anodes and b) their respective carbon positive electrodes after the chemical stability which correspond to the SEM images in Figure 4.

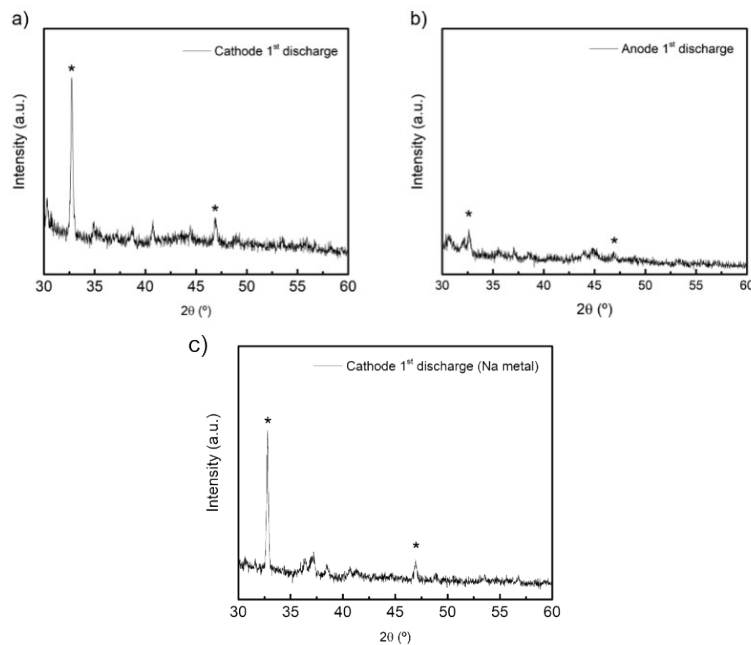


Figure S14. XRD patterns of the cathode discharge with Sn₄P₃ alloy (a) and the corresponding anode (b); and the cathode discharge with Na metal anode (c).

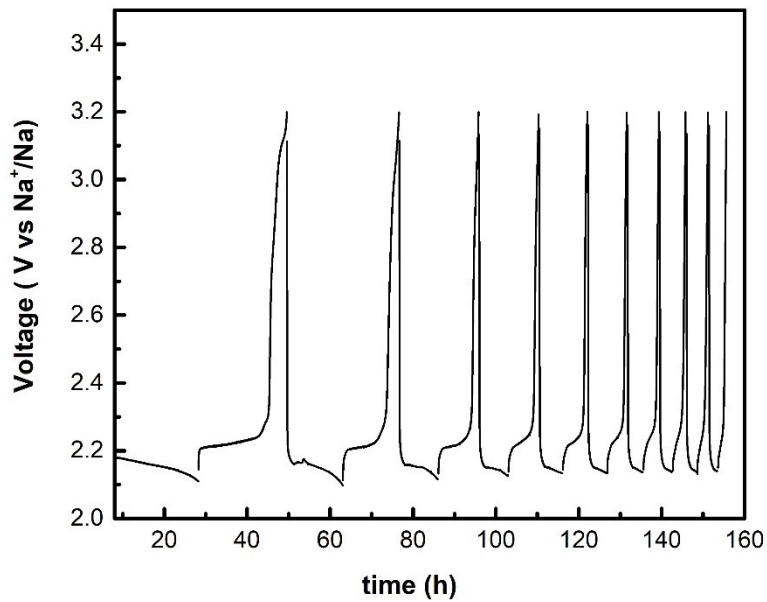


Figure S15. Galvanostatic cycling of the alloy during EIS measurements of the Sn₄P₃/C//GDL cell.